Computation of Cavity Shapes, Sizes, and Plasticities

PETER COMBA, NORBERT OKON, RAINER REMENYI

Anorganisch-Chemisches Institut, Universität Heidelberg, Im Neuenheimer Feld 270, D69120 Heidelberg, Germany

Received 23 November 1998; accepted 15 January 1999

ABSTRACT: A new molecular mechanics approach has been developed and used to scan the optimum geometry (size and shape) of a host molecule and the energy cost for the deformation of the bonding cavity, based on a general, unspecific guest with given docking sites and a variable size. Lagrange multipliers are used to constrain the sum of internal coordinates (host–guest docking-site distances), and no assumptions with respect to the type and strength of the host–guest bonding have to be made. This new approach has been fully implemented in a molecular mechanics program, and it is used to compute the size, shape, and plasticity of a rigid, asymmetrical, tetradentate $(N_{amine})_2(N_{pyridine})_2$ ligand. It is shown that all other methods for the computation of ligand hole sizes that have been reported so far are not able to compute the ligand cavities independently of the metal ion, and they lead to strikingly different shapes, sizes, and plasticities.
J Comput Chem 20: 781–785, 1999

Keywords: hole sizes; metal ion selectivity; cavity shape; plasticity; preorganization

Introduction

The size, shape, and plasticity (deformability) of binding sites are important factors in selective host–guest interactions. Applications range from biological systems to industrial catalysis (key–lock principle,[1] entatic state,[2,3] and induced-fit models[4,5]), and from medical applications to metal ion discrimination (docking of substrates and inhibitors,[6] rational drug design,[7] and ligand preorganization[8–10]). Size and shape selection has been a major factor in this field, particularly where the directionality of the host–guest bonding is relatively unimportant—that is, where the interactions are based primarily on electrostatics and/or hydrogen bonding. Size (and shape) selectivity in the area of metal ion discrimination has often been overinterpreted, especially, when transition metal

Correspondence to: P. Comba; e-mail: comba@akcomba.oci.uni-heidelberg.de

Contract/grant sponsors: German Science Foundation; Fonds of the Chemical Industry

CCC 0192-8651 / 99 / 080781-05

ions with specific electronic effects (directionality and relative strength of metal donor bonding) are involved, and this has been discussed in detail elsewhere.[10] Nevertheless, ligand preorganization and ligand complementarity (i.e., the size, shape, and plasticity of the metal-free ligand system) is one of the important factors in this area. Also, due to the specific and variable metal ion-based influences, it is especially important to evaluate the properties of ligand-bonding cavities independently of the metal ion.

A number of primarily molecular mechanics-based approaches for the computation of ligand ''hole sizes'' have been proposed, but none is truly metal ion independent, and none is able to compute accurately asymmetrical ligand cavities. All are based on the metal−donor (M−L) potential which, in its harmonic form, is given by:

$$E_{M-L} = \frac{1}{2} k_{M-L} (r_{M-L} - r^0_{M-L})^2 \qquad (1)$$

Plots of the strain energy ($E_{M\text{-}L}$) as a function of the hole size ($r_{M\text{-}L}$) have been produced by varying the ideal (or undeformed) metal−donor distance, $r^0_{M\text{-}L}$, or by scanning the effective distance $r_{M\text{-}L}$ with restraints (exceedingly large force constants, $k_{M\text{-}L}$) or constraints (Lagrange multipliers). Much data have been produced using these methods; they have been reviewed extensively[10−18] and debated.[10,17,19,20] In the most general approach presented so far, metal ion independence was obtained by constraining the metal−donor bonds $r_{M\text{-}L}$ with Lagrange multipliers, by setting the corresponding force constants ($k_{M\text{-}L}$) to zero, and by replacing the donor−metal−donor (L−M−L) bending terms by 1,3-nonbonded interactions (points-on-a-sphere model; metal−donor−substituent [M−L−R] bending was assumed to have a constant force).[17,21,22] It was pointed out, however, that metal-ion-selective ligands are usually asymmetrical and, therefore, the corresponding metal−donor bonds may not be varied uniformly.[16] So far, no general method to address this problem has been made available.

We now present a new model in which we use a dummy atom (unspecific metal ion) in the center of the ligand cavity and vary its size by constraining the *sum* of all metal−donor (M−L) distances. The angular distribution of the donors is determined by van der Waals forces (points-on-a-sphere model). This scenario allows each donor to react individually to the stresses of the cavity; that is, the ''blowing up'' of the cavity is similar to that of a balloon with uneven rubber walls. This model is used to compute the shape, size, and plasticity of the rigid tetradentate bispidine-type ligand shown in Figure 1, and the computed size, shape, and plasticity of the ligand cavity is discussed in detail and in comparison with results of ''hole-size'' computations obtained with conventional methods.[23]

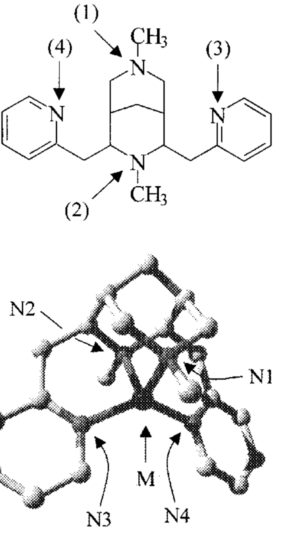

FIGURE 1. Structure of the substituted bispidine ligand and of its tetracoordinated metal compound.

Computational Details

The MOMEC program[24] and parameterization scheme[25] were used for all computations. This is a rather conventional diagonal force field, based on harmonic functions and a Buckingham potential for the van der Waals interactions. Donor−metal−donor forces[26] were all set to zero (points-on-a-sphere model).[22,25] Details of the potential energy functions and parameter sets have been given elsewhere.[16,17,22,24−26] The full-matrix Newton−Raphson algorithm was used for strain energy minimization and Lagrangian multipliers were applied to constrain the sum of internal coordinates (i.e., all metal [dummy atom]−donor bonds).[27−31] The constraints are given by:

$$c(r_{ab}) = \sum r_{ab} + S = 0 \qquad (2)$$

where c is the constraint, r_{ab} are bond distances between two atoms with constrained distances, and S is the sum of all constrained bond distances.

In internal coordinates this is:

$$c(x_{ik_l}) = \sum_{l=1\ldots n}\left((x_{a1_l} - x_{b1_l})^2 + (x_{a2_l} - x_{b2_l})^2 + (x_{a3_l} - x_{b3_l})^2\right)^{\frac{1}{2}} + S = 0 \quad (3)$$

where x_{ai_l}, x_{bi_l} are Cartesian coordinates of two atoms bound to each other at a constrained distance. The Lagrange function is given by:

$$L(\mathbf{x}, \boldsymbol{\lambda}) = E(\mathbf{x}) - \boldsymbol{\lambda} c(\mathbf{x}) \quad (4)$$

where L is the Lagrange function, E is the potential energy function, $\mathbf{x}$ is the vector of all Cartesian coordinates, and $\boldsymbol{\lambda}$ is the vector of all Lagrangian multipliers. The gradient vector and the Hessian matrix are given by:

$$\nabla L(\mathbf{x}, \boldsymbol{\lambda}) = \begin{pmatrix} \nabla_x(E + \boldsymbol{\lambda} c) \\ \nabla_\lambda \boldsymbol{\lambda} c \end{pmatrix} \quad (5)$$

$$\mathbf{H}(\mathbf{x}, \boldsymbol{\lambda}) = \begin{bmatrix} \nabla_x^2 E - \sum_i \nabla_x \boldsymbol{\lambda} c & \nabla_{x,\lambda} \boldsymbol{\lambda} c \\ \nabla_{x,\lambda}{}^T \boldsymbol{\lambda} c & 0 \end{bmatrix} \quad (6)$$

where $\nabla L(\mathbf{x}, \boldsymbol{\lambda})$ is the gradient vector of the Lagrange function and $\mathbf{H}(\mathbf{x}, \boldsymbol{\lambda})$ is the Hessian matrix of the Lagrange function. The shift to all coordinates and the following iteration step are given by:

$$\begin{pmatrix} \partial \mathbf{x} \\ \boldsymbol{\lambda} \end{pmatrix} = \begin{pmatrix} \nabla_x E \\ \nabla_\lambda \boldsymbol{\lambda} c \end{pmatrix} \mathbf{H}(\mathbf{x}, \boldsymbol{\lambda})^{-1} \quad (7)$$

$$\mathbf{x}^{r+1} = \mathbf{x}^r + \partial \mathbf{x} \quad (8)$$

where $\partial \mathbf{x}$ is the shift of the Cartesian coordinates and r is the number of iterations.

No metal-ion-dependent parameters were used in the calculations (M–N–R angle bending potentials are assumed to be metal ion independent; k_θ(M–N$_{amine}$–R) = 0.2 mdyn Å rad^{-2}, k_θ(M–N$_{pyridine}$–R) = 0.2 mdyn Å rad^{-2}, θ^0(M–N$_{amine}$–R) = 1.920 rad, θ^0(M–N$_{pyridine}$–R) = 2.094 rad).[25]

Results and Discussion

The bonding cavity of the bispidine-type ligand shown in Figure 1 has been computed with three methods. All involved constraints for the four metal–donor (M–L) bonds and the potential energies for the metal–donor bonds were set to zero ($k_{M\text{-}L}$ = 0.0) in all three models. Metal ion independence was further achieved by setting the valence-angle-bending potentials around the metal ion (donor–metal–donor terms) to zero and by using a constant force for the two types of valence angle bending around the donor atoms in the three types of calculation (see previous section). 1,3-Nonbonded interactions around the metal ion (i.e., donor atom–donor atom van der Waals interactions) were applied in all three models. This is a general method to model the angular distribution of the donors around a metal center (points-on-a-sphere approach).[17,22,32] Also, in the new approach presented here, where the cavity size is scanned independently of the metal ion (variation of the cavity size without any metal ion present, see "method C" [*sum*] in what follows) the donor atom–donor atom interactions are normal van der Waals interactions and, for comparison, they were also included in the other two approaches.

In method A *(sym)*, all four bonds were varied symmetrically; that is, for each point on the strain energy versus averaged metal–donor bond distance (r_{av}) curve (see Fig. 2), all four bonds have the same distance (starting point: M–L = 1.5 Å; endpoint: M–L = 2.5 Å; step size: 0.03 Å).

In method B *(asym)*, the four metal–donor (M–L) distances were varied independently. Various methods are possible to define the individual starting values and step sizes,[16,23] but all are based on: (i) the computation of specific metal complexes (in the published work on the bispidine-type ligand considered here, the corresponding Co^{III}, Cr^{III}, low-spin Fe^{III}, Co^{II}, and Cu^{II} complexes were optimized[23])—that is, a certain metal ion dependence is introduced in this step; and (ii) the assumption that each individual metal–donor bond distance varies linearly. The corresponding curve in Figure 2 was obtained as described earlier, with the following parameters (M–N1, M–N2, M–N3, M–N4, respectively). Starting point: 1.868, 1.862, 1.844, 1.844 Å; step size: 0.0224, 0.0192, 0.0204, 0.0204 Å; endpoint: 2.14, 2.11, 2.11, 2.11 Å; (Fig. 1).

In method C *(sum)*, the new module with sum constraints was used and the average metal–donor distance (i.e., one fourth of the actual sum) was varied from 1.5 to 2.5 Å; with a step size of 0.03 Å.

From Figure 2, it can be seen that the two curves based on method A (*sym*) and method B (*asym*) are practically identical. Based on similar studies with other ligand systems this is somewhat surprising. However, the asymmetry induced by method B is comparably small (see earlier) and, because metal center–donor terms are removed from the total energy, the major structural differences are changes in ligand-backbone-based torsional angles. These generally have rather shallow

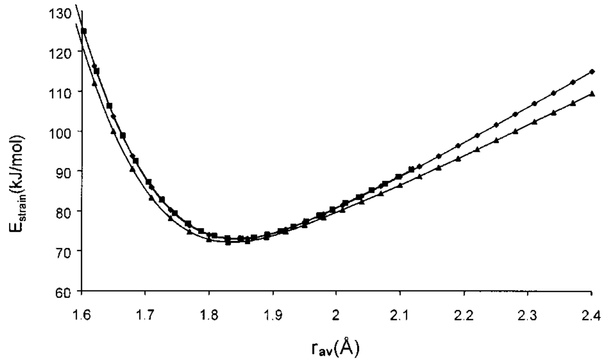

FIGURE 2. Computed strain energy as a function of the averaged metal–donor bond distance for the three models discussed in the text (squares: *sym*; diamonds: *asym*; triangles: *sum*).

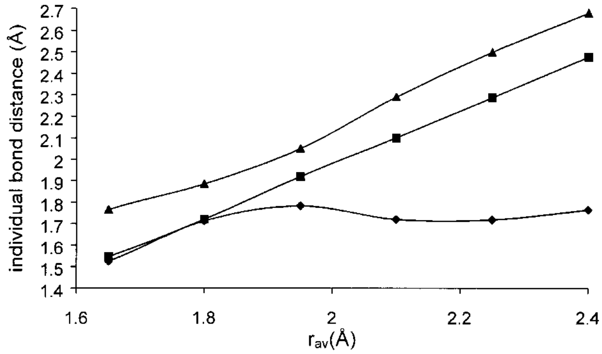

FIGURE 3. Plot of the three individual metal–donor distances (M–N3 and M–N4 are identical) vs. the averaged M–L distance (triangles: M–N1; diamonds: M–N2; squares: M–N3,4) using method C, (*sum*).

potential energy surfaces. The observation that the two curves based on methods A (*sym*) and B (*asym*) are very similar demonstrates that the determination of metal-dependent start and end values and the linear interpolation between these parameters might represent a poor approximation.

More noteworthy is the observation that the third curve, which is based on method C (*sum*), generally has the lowest strain energy. This indicates that, at the energy minimum (r_{av} = 1.835 Å, E_{strain} = 72.2 kJ/mol), the cavity is in its lowest strain geometry; that is, lower than at each point of the two other curves (the corresponding M–L distances [distances to the dummy atom] are: M–N1 = 1.752, M–N2 = 1.766, M–N3 = 1.911, M–N4 = 1.911 Å; note that this may not be the preferred metal-free ligand conformation, because donor lone pairs are forced to be directed toward the center of the cavity). The computed structures based on methods A and B (*sym* and *asym*) are generally more strained, and this is due to stresses enforced by an arbitrary distribution of M–L bond distances. That is, the choice of metal-ion-dependent start and end values and/or a linear variation of the four metal–donor distances are unrealistic assumptions. The latter point is illustrated in Figure 3, in which the four individual bond distances are plotted against the enforced cavity size (i.e., the average M–L distance in method C [*sum*]; the distances to the two pyridine donors N3 and N4 are, as expected, identical). It can be seen that the two pyridine donors enforce a displacement of the metal center from the center of the cavity, and this is strongly (and not linearly) dependent on the metal ion size.

The fact that this asymmetry is modulated by specific metal ions indicates that only the computation of the cavity shape, size, and plasticity by the approach based on sum constraints leads to a realistic, metal-ion-independent result. This interpretation is based not only on the fact that the computed minimum structures and strain energies are significantly different (method C [*sum*]: r_{av} = 1.835 Å, E_{strain} = 72.2 kJ/mol; methods A and B [*sym*, *asym*]: r_{av} = 1.845 Å, E_{strain} = 73.0 kJ/mol) and that there are small differences in the relative steepness of the curves. The most important difference is the striking change in structural features. At an average M–L distance r_{av} = 2.10 Å, the distances to the metal ion (method B, *asym*) and to the dummy atom (method C, *sum*) are: M–N1 = 2.10, 2.29 Å; M–N2 Å; 2.12, 1.72 Å; M–N3,4 = 2.09, 2.10 Å, respectively. Thus, as expected (see earlier text and Fig. 3), the changes in the cavity shape and plasticity are strongly modulated by a metal ion. An important feature is that the relative bond strengths and distances to pyridine and amine donors are metal ion dependent. This also emerges from a comparison with a "real" computed complex, that of cobalt(II), which has the same averaged metal–donor distance (r_{av} = 2.1025 Å, Co–N1 = 2.14, Co–N2 = 2.09 Å, Co–N3,4 = 2.09 Å).[23]

What is the significance of a truly metal-ion-independent computation of the cavity size, shape, and plasticity? It is a quantitative measure for the stress induced by the ligand on the metal ion and, therefore, is also a measure for the degree of preorganization or complementarity of a ligand system with respect to a specific metal complex. However, it does not necessarily give a realistic indication of

metal ion discrimination by a ligand system, because metal ion–donor atom bonding (i.e., electronic effects) is not explicitly included in ''hole size'' calculations. This also emerges from the fact that the modulation of the metal–donor distance distribution is strongly dependent on the preferences of the specific metal ion. This is especially important for transition metal centers, but less important for alkali, alkaline earth, and rare earth compounds.

Conclusions and Outlook

The computation of strain energies as a function of metal–donor distances has often been used to compute bonding cavity sizes. The method presented here is the first that is fully metal ion independent and also able to deal with asymmetrical ligands. It therefore may be used to accurately compute the size, shape, and plasticity of bonding cavities. Similar methods have been used in molecular mechanics-based approaches to compute electron transfer rates of transition metal ion coordination compounds.[33] In those types of studies, the metal–donor bonding potentials need to be included, and this is possible with the method presented here. Sum constraints may also be defined for other internal coordinates, that is, for valence and torsional angles, but these have not yet been implemented in our software. Possible applications of these constraints include scanning of the potential energy surfaces of tetracoordinate compounds along a tetrahedral twist mode (square planar vs. tetrahedral coordination geometry) and similar geometric interconversions for five- and six-coordinate metal complexes (Berry twist and Bailar twist, respectively).

The computation of shapes, sizes, and flexibilities of bonding cavities is of increasing importance in the field of host–guest chemistry in general, and in many applications in biological and medical systems. The approach based on the constraint of the sum of internal coordinates may lead to new, simpler methods for the interpretation of the interactions between various types of host and guest molecules.

References

1. Fischer, E. Chem Ber 1984, 27, 2985.
2. Lumry, R.; Eyring, H. J Phys Chem 1954, 58, 110.
3. Vallee, B. L.; Williams, R. J. P. Proc Natl Acad Sci USA 1968, 59, 498.
4. Yankeelov, J. A., Jr.; Koshland, D. E. J Biol Chem 1965, 240, 1593.
5. Cleland, W. W. Acc Chem Res 1975, 8, 145.
6. Kaim, W.; Schwederski, B. Bioanorganische Chemie; Teuber: Stuttgart, 1995.
7. Doucet, J.-P.; Weber, J. Computer-Aided Molecular Design: Theory and Applications; Academic: London, 1996.
8. Cram, D. J.; Kamda, T.; Helgeson, R. L.; Liu, G. M. J Am Chem Soc 1979, 99, 948.
9. Cram, D. J.; Liu, G. M. J Am Chem Soc 1985, 107, 3657.
10. Comba, P. Coord Chem Rev. In press.
11. Henrick, K.; Tasker, P. A.; Lindoy, L. F. Progr Inorg Chem 1985, 33, 1.
12. Hancock, R. D. Acc Chem Res 1990, 23, 253.
13. Drummond, L. A.; Hendrick, K.; Kanagasundaram, M. J. L.; Lindoy, L. F.; MacPartlin, M.; Tasker, P. A. Inorg Chem 1982, 21, 3923.
14. Henrick, K.; Lindoy, L. F.; McPartlin, M.; Tasker, P. A.; Wood, M. P. J Am Chem Soc 1984, 106, 1641.
15. Lindoy, L. F. Progr Macrocycl Chem (Izatt Ed) 1986, 33, 53.
16. Comba, P.; Hambley, T. W. Molecular Modeling of Inorganic Compounds; VCH: Weinheim, 1995.
17. Comba, P. Coord Chem Rev. 1993, 123, 1.
18. Busch, D. H. Acc Chem Res 1978, 11, 392.
19. Drew, M. G. B.; Yates, P. C. J Chem Soc Dalton Trans 1986, 2505.
20. Hancock, R. D. J Chem Soc Dalton Trans 1986, 2505.
21. Comba, P. Inorg Chem 1989, 28, 426.
22. Bernhardt, P. V.; Comba, P. Inorg Chem 1992, 31, 2638.
23. Comba, P.; Nuber, B.; Ramlow, A. J Chem Soc Dalton Trans 1997, 347.
24. Comba, P.; Hambley, T. W.; Okon, N.; Lauer, G. MOMEC, A Molecular Modeling Package for Inorganic Compounds; CVS: Heidelberg, 1997. E-mail:cvs@t-online.de.
25. Bol, J. E.; Buning, C.; Comba, P.; Reedijk, J.; Ströhle, M. J Comput Chem 1998, 19, 512.
26. Comba, P.; Hambley, T. W.; Ströhle, M. Helv Chim Acta 1995, 78, 2042.
27. Boyd, R. H. J Chem Phys 1968, 49, 2574.
28. Fletcher, R. Practical Methods of Optimization; Wiley: New York, 1997.
29. Thomas, M. W.; Emerson, D. J Mol Struct 1973, 16, 473.
30. van de Graaf, B.; Baas, J. M. A. Recl Trav Chim Pays-Bas 1980, 99, 327.
31. Wiberg, K. B.; Boyd, R. H. J Am Chem Soc 1972, 8426.
32. Hambley, T. W.; Hawkins, C. J.; Palmer, J. A.; Snow, M. R. Austral J Chem 1981, 34, 45.
33. Comba, P.; Sickmüller, A. F. Inorg Chem 1997, 36, 4500.